FEBS Letters 586 (2012) 1622–1630

FEBS Letters

journal homepage: www.FEBSLetters.org

Catalytic promiscuity in *Pseudomonas aeruginosa* arylsulfatase as an example of chemistry-driven protein evolution

Jinghui Luo [a,b], Bert van Loo [c], Shina C.L. Kamerlin [a,*]

[a] Department of Cell and Molecular Biology (ICM), Uppsala University, Uppsala Biomedical Center, Box 596, S-751 24 Uppsala, Sweden
[b] Department of Biophysical and Structural Chemistry, Leiden Institute of Chemistry, Leiden University, 2300 RA Leiden, The Netherlands
[c] Department of Biochemistry, University of Cambridge, 80 Tennis Court Road, CB2 1GA Cambridge, United Kingdom

ARTICLE INFO

Article history:
Received 29 February 2012
Revised 30 March 2012
Accepted 9 April 2012
Available online 25 April 2012

Edited by Miguel De la Rosa

Keywords:
Enzyme catalysis
Empirical valence bond
Phosphoryl transfer
Sulfuryl transfer
Electrostatic reorganization

ABSTRACT

In recent years, it has become increasingly clear that many enzymes are catalytically "promiscuous". This can provide a springboard for protein evolution, allowing enzymes to acquire novel functionality without compromising their native activities. We present here a detailed study of *Pseudomonas aeruginosa* arylsulfatase (PAS), which catalyzes the hydrolysis of a number of chemically distinct substrates, with proficiencies comparable to that towards its native reaction. We demonstrate that the main driving force for the promiscuity is the ability to exploit the electrostatic preorganization of the active site for the native substrate, providing an example of chemistry-driven protein evolution.

1. Introduction

The classic textbook view: 'One enzyme, one activity' is being challenged by mounting evidence that many enzymes are capable of catalyzing chemically distinct conversions by stabilizing different transitions states (TSs) [1]. The existence of such catalytic "promiscuity" provides a potential explanation as to how enzymes with new activities can evolve from existing ones [2], since a previously absent activity in a protein scaffold has a very low likelihood of being introduced with only a few mutations. Promiscuity is therefore also important for enzyme design, as it can provide an immediate selective advantage by providing an initially weak activity that can be improved by mutation in future generations. This is significant, as it has proven extremely difficult to design new enzymes de novo, and even using existing scaffolds to accommodate novel active sites (e.g. [3]), though impressive, has had limited success in terms of the catalytic proficiency of the resulting constructs.

Although there are an increasing number of reports on (catalytic) promiscuity in recent years, many of these are anecdotal and systematic studies on the subject are rare. A superfamily for which the phenomenon of 'crosswise promiscuity' is well studied is the alkaline phosphatase (AP) superfamily, in which the primary activity of one family member is often a promiscuous activity in another [4], and the reactions catalyzed by the AP-superfamily members are amongst the most thermodynamically demanding known [5]. One of these superfamily members for which the promiscuous behavior is well described is *Pseudomonas aeruginosa* arylsulfatase (PAS) [6,7], for which both the catalytic proficiencies $((k_{cat}/K_M)/k_{uncat})$ and amplification (k_{cat}/k_2) for some of the promiscuous side activities can almost rival those of its primary reaction [6], making it a good model system to study the molecular basis for enzyme specificity and promiscuity.[1]

In the present work, we present a detailed theoretical analysis of the catalysis of sulfate and phosphate ester hydrolysis by PAS. The selected substrates are chemically distinct, varying in both size, charge and protonation requirements [8], and yet PAS is capable of catalyzing all of them with surprisingly high efficiency and low discrimination [6]. Our calculations strongly suggest that for sulfate monoester hydrolysis, the reaction proceeds via concerted nucleophile deprotonation by a nearby histidine, whereas in the case of the phosphoryl transfer reactions, the phosphate itself is capable of acting as a base, in analogy to a number of other

* Corresponding author. Fax: +46 (18) 471 2000.
E-mail address: kamerlin@icm.uu.se (S.C.L. Kamerlin).

[1] Note that k_2 here refers to the rate of the uncatalyzed reaction when 55 M concentration effects have been taken into account. Additionally, we distinguish between catalytic proficiency and amplification, as the catalytic amplification highlights the catalytic power of the enzyme (taking into account how "difficult" the uncatalyzed reaction is), whereas, at a given substrate concentration, the amount of product produced is determined by the catalytic efficiency, or k_{cat}/K_M.

0014-5793/$36.00
http://dx.doi.org/10.1016/j.febslet.2012.04.012

phosphatases (see e.g. [9], and references cited therein). We additionally propose that the ionization state of an active site lysine, Lys113, which interacts with one of the non-bridging oxygens of the substrate, is important for determining the specificity of the enzyme (as would also be hinted at by the experimentally observed pH profiles [7]). Finally, a comparative analysis of the electrostatic contributions of different residues to the overall activation barrier demonstrates that the driving factor controlling the promiscuity is the electrostatic preorganization of the active site, providing a strong argument in favor of chemistry-driven protein evolution.

2. Materials and methods

Our study first thoroughly characterized the background reactivity in aqueous solution using a combination of experimental data for analogous reactions as well as constructing the appropriate *ab initio* free energy surfaces, as outlined in the SI Text. Subsequent empirical valence bond (EVB) calculations were performed using the MOLARIS simulation package and the ENZYMIX forcefield [10], with EVB activation barriers being obtained using the standard free energy perturbation/umbrella sampling (FEP/US) approach outlined in [11]. The initial atomic coordinates for *P. aeruginosa* arylsulfatase at 1.3 Å resolution [12] were obtained from the Protein Data Bank [13] (accession code 1HDH). In each case, the relevant substrate was placed into the active site by manually overlaying it over our positioning of *p*-nitrophenyl phosphate in our previous study [14], and the resulting complex was then first relaxed for 30 ps at 30 K, followed by 100 ps at 300 K, using a 1 fs timestep. Two independent relaxation runs were performed with Lys113 in either its ionized or neutral state, all other ionization states were assigned as in [14]. Initial structure relaxation was performed using a 24 Å water sphere, centered on the substrate and surrounded by first a 3 Å grid of Langevin dipoles, and then by bulk solvent (which was modeled using the surface constrained all atom solvent model (SCAAS) [10]). Long-range effects were treated using the local reaction field (LRF) approach [15]. Once structure relaxation was complete, a smaller 20 Å explicit water sphere was used for the actual EVB/FEP-US simulations, which was extended first to 22 Å with a grid of Langevin dipoles, and then to infinity with bulk solvent. The FEP mapping was performed in 51 mapping frames of 50 ps each in length, giving a total simulation time of 2.55 ns per trajectory, and all simulations were repeated ten times with different initial conditions. Finally, the electrostatic contributions of different residues to the overall activation barrier were evaluated using the linear response approximation (LRA), in line with our previous study [14].

3. Results

3.1. Native sulfatase activity

In aqueous solution, the hydrolyses of the *p*-nitrophenyl sulfate (pNPS) and phosphate (pNPP) monoesters proceed with similar kinetics, leading to the suggestion that the hydrolysis of the two compounds proceeds through similar transition states (Fig. SI, [16]). However, we have shown [8] that, in the uncatalyzed reaction, pNPS hydrolysis proceeds through a noticeably more expansive transition state than pNPP hydrolysis, with very different solvation effects. Additionally, pNPP hydrolysis appears to proceed via a substrate-as-base mechanism, in which a proton from the attacking water molecule is transferred to the phosphate dianion, which is acting as a "proton sink", to generate hydroxide and a phosphate monoanion (note that we found this to happen both in aqueous solution and PAS [8,14]). However, this mechanism is not available to the analogous sulfate monoester, due to the significantly lower pK_a (<−3) of its non-bridging oxygens (see [14] and references cited therein). Such differences have dramatic implications for reactions in the tightly optimized environment of an enzyme's active site, making it particularly surprising that PAS is even able to catalyze such chemically distinct substrates.

Fig. 1 highlights the proposed mechanism for acid-base catalyzed sulfate monoester hydrolysis by PAS [7,12]. The sulfate monoester is unlikely to act as a proton acceptor and our earlier study [14] ruled out the nearby Asp317. An alternative proton acceptor is His115, which has been suggested to be the general base for the subsequent hemiacetal cleavage [7,12] (see Fig. S2 for the orientation of these residues). Therefore, here, we have explored the energetics of a potential mechanism involving concerted-proton transfer from the geminal diol to His115. Extrapolating from literature values for the spontaneous and base-catalyzed hydrolyses of pNPS in aqueous solution under different buffer conditions suggests that the activation barrier for nucleophilic attack by the corresponding geminal diol in solution would be expected to be ∼28.5 kcal/mol, based on a pK_a of ∼13.5 for the geminal diol (see [14] and the SI text). We obtain a similar activation barrier when also taking into account the potential chemical effect of general base-catalysis by the imidazole group (Table SI), which *ab initio* calculations (Fig. S3) suggest proceeds *via* a single concerted transition state, with the histidine being the ultimate proton acceptor. Finally, adjusting for 55 M water concentration effects gives a $\Delta g^{\neq}_{cage}$ of ∼26.3 kcal/mol (for a discussion of $\Delta g^{\neq}_{cage}$, see e.g. [17]). The experimentally measured k_{cat} for the sulfuryl transfer reaction catalyzed by PAS at 25 °C and pH 8.0 [7] is 14.2 s^{-1}, yielding an activation barrier ($\Delta g^{\neq}_{enz}$) of ∼15.9 kcal/mol, and therefore, the catalytic amplification (i.e. $\Delta g^{\neq}_{enz} - \Delta g^{\neq}_{cage}$) for the native sulfatase activity compared to the relevant reference reaction in aqueous solution is estimated to be ∼10.4 kcal/mol.

A significant issue is the discrepancy between the pH dependence of k_{cat}/K_M for the native sulfatase and promiscuous phosphomonoesterase activities of PAS (Fig. 7 of [7]). That is, while the apparent pK_a value for the native sulfatase activity is ∼8.3, the corresponding value for the phosphatase activity is much lower than this, and it was postulated [7] that the difference between the two pH rate profiles can be a result of the differential protonation of active site residues responsible for binding substrates differing by a total charge unit. Examination of the PAS active site suggests that the best candidate for this shift would be Lys113, which interacts with one of the non-bridging oxygens of the substrate (Fig. S2), provided its pK_a is depressed from the corresponding value in solution (∼10.5). This could be the case due to its close vicinity to the Ca^{2+} ion in the active site (Fig. S2). To test this, we evaluated the pK_a of this residue using the semi-macroscopic protein dipoles-Langevin dipoles (PDLD/S-LRA) approach [18], obtaining pK_a values in the range of 5.7–7.9, over a range of dielectric constants between 8 and 12 (see Discussion in [19]). In the absence of experimental data, these calculations only make a qualitative and not a quantitative prediction; however, they suggest that a change of preferred protonation state of Lys113 between the sulfatase and phosphatase activities is at least feasible, and that at pH 8 (at which the experimental k_{cat} was measured), this residue could be in either ionization state. Therefore, we separately relaxed PAS with Lys113 in either its ionized ($Lys113^+$) or neutral ($Lys113^0$) state, and used the resulting structures as starting points for subsequent EVB calculations. Additionally, as shown in Fig. S2, the orientation of the nucleophile relative to His115 is such that it is unlikely that direct proton transfer occurs from the nucleophilic oxygen atom to the histidine. However, as the hydroxyl groups of the geminal diol are chemically identical, it is entirely plausible that the nucleophile is activated via a double proton transfer in

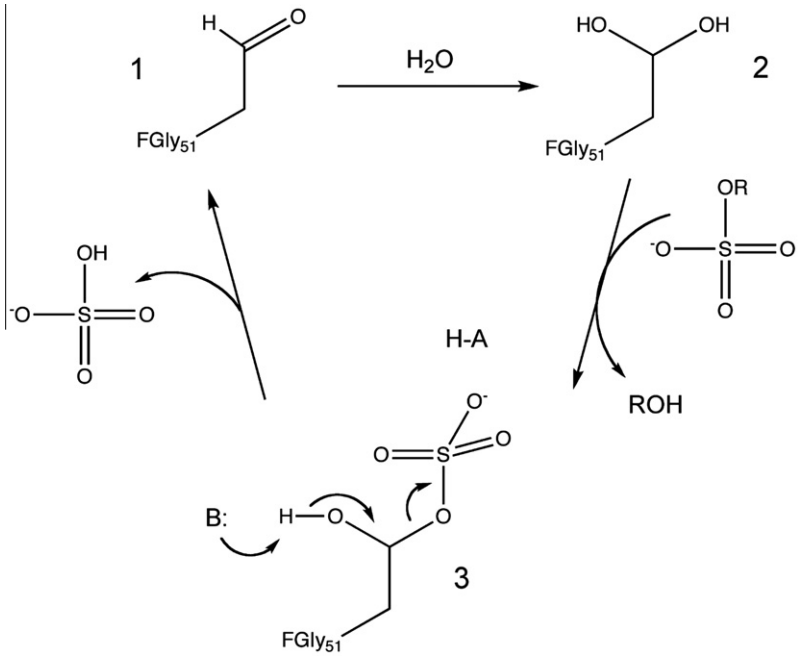

Fig. 1. Proposed mechanism for the native sulfatase activity of *P. aeruginosa* arylsulfatase (PAS) [6,12]. (1 → 2) represents the attack of a water molecule on an aldehyde to form the corresponding nucleophilic aldehyde hydrate i.e. geminal diol, FGly51, see also the SI), (2 → 3) represents subsequent nucleophilic attack on the sulfate with concomitant leaving group departure (occurring in a single concerted transition state), and, finally, (3 → 1) represents hemiacetal cleavage to release the phosphate and regenerate the geminal diol.

Table 1
EVB parameters, calculated activation and free energies and reorganization energies for the relevant group transfers.

System[a]	H_{12}[b]	α_0[b]	$\Delta g^{\neq}_{calc}$[c]	$\Delta G_{0,calc}$[c]	$\Delta g^{\neq}_{exp}$[d]	λ[e]	$\Delta g^{\neq}_{cage} - \Delta g^{\neq}_{enz}$[f]
(Ia)							
Water	395.0	21.5	26.3(0.2)	−5.5(0.2)	26.3	933.3(11.9)	
$Lys113^+$			18.4(1.0)	−1.9(1.3)		809.1(4.5)	
$Lys113^0$			15.3(1.6)	−10.7(3.7)	15.9	821.8(3.4)	11.0
(Ib)							
Water	313.5	26.0	26.3(0.2)	−5.5(0.2)	~26−27	856.0(13.6)	
$Lys113^+$			22.8(0.9)	−7.0(1.2)		742.9(6.0)	
$Lys113^0$			18.8(1.4)	−11.3(2.2)	15.9	755.8(2.7)	7.5
(2)							
Water	363.0	−38.4	24.6(0.9)	−2.1(1.4)	24.7	833.4(8.7)	
$Lys113^+$			30.5(1.9)	19.0(2.0)		738.1(6.4)	
$Lys113^0$			20.4(0.3)	0.2(0.8)	19.0	741.0(2.7)	4.4
(3)							
Water	340.0	−14.5	26.9(1.1)	0.9(1.6)	26.9	822.6(5.0)	
$Lys113^+$			32.0(1.2)	18.7(2.4)		742.8(2.6)	
$Lys113^0$			16.7(0.3)	−0.1(1.2)	17.8	762.5(7.1)	10.2
(4)							
Water	310.0	−40.0	27.3(0.3)	−10.4(1.4)	~27.0	806.7(7.6)	
$Lys113^+$			19.5(1.1)	−12.7(2.2)	19.6	722.4(4.7)	7.8
$Lys113^0$			13.5(1.4)	−26.2(2.7)		737.3(6.0)	

[a] (1) *p*-nitrophenyl sulfate (associative (a) and dissociative (b) pathways), (2) ethyl-*p*-nitrophenyl sulfate, (3) bis-*p*-nitrophenyl sulfate and (4) *p*-nitrophenyl phosphate.
[b] H_{12} and α_0 denote the off-diagonal element of the EVB Hamiltonian and the gas-phase shift of the product state respectively (which appears in the H_{22} element of the EVB Hamiltonian). The gas-phase shift in the reactant state H_{11} is zero in all cases.
[c] Calculated activation energies and reaction free energies, in kcal/mol.
[d] Experimentally observed activation free energies, in kcal/mol. The activation free energy in solution is estimated as discussed in the main text.
[e] Total reorganization energies, λ, in kcal/mol.
[f] Calculated catalytic enhancement, in kcal/mol, relative to the reference reaction in aqueous solution, for the preferred ionization state of Lys113 (see main text). Values in parentheses denote standard deviations over ten trajectories.

which the proton on the nucleophilic oxygen is transferred to the other oxygen of the geminal diol, the proton on which is in turn transferred to Hisll5 (see Fig. S4). Finally, the *ab initio* surface (Fig. S3) suggests there is no need for protonation of the leaving group and therefore no need for a general acid during the chemical step.

The relevant valence bond structures for this proposed mechanism are shown in Fig. S4, the EVB parameter set used is shown in

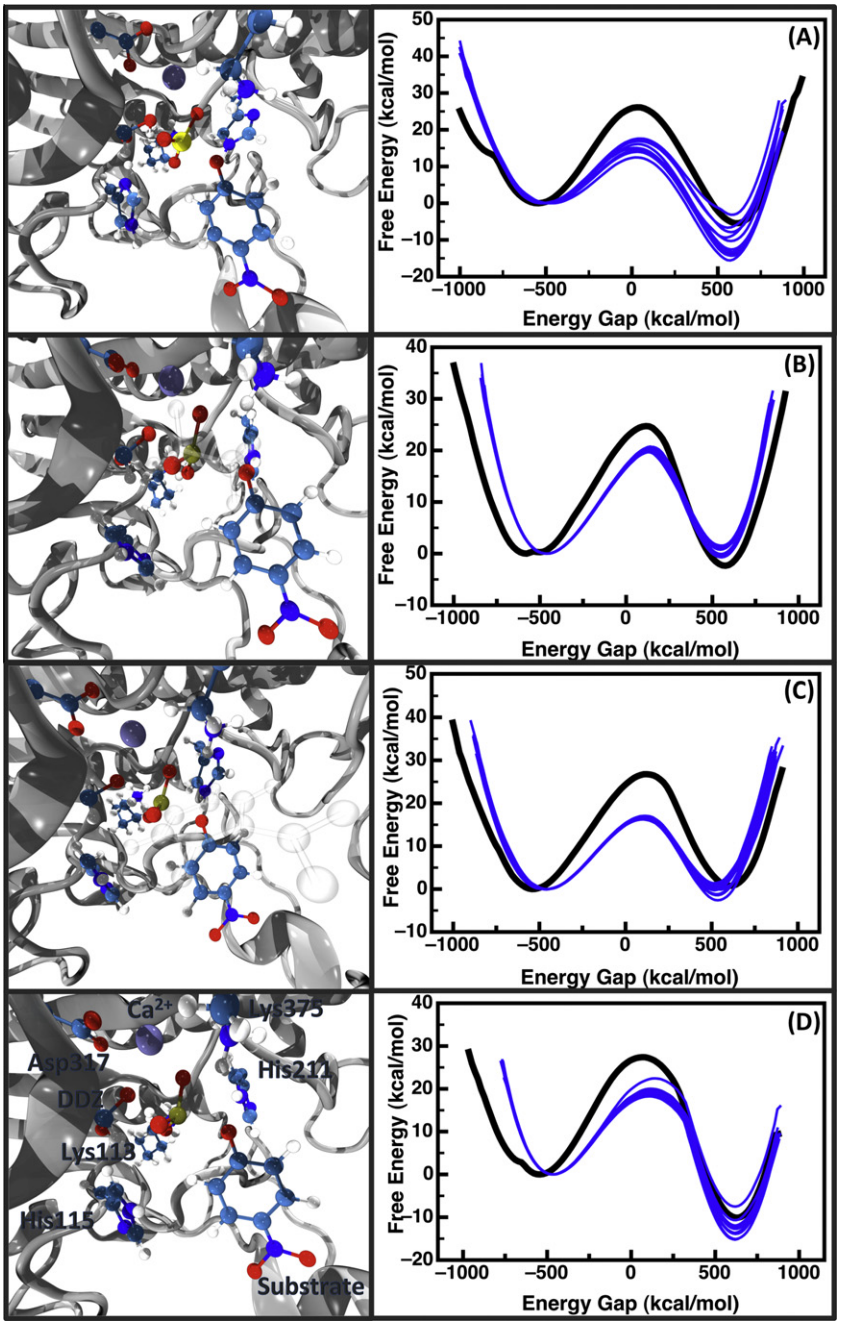

Fig. 2. Empirical valence bond (EVB) free energy profiles in enzyme (blue) and in solution (black), as well as representative transition state geometries for the enzymatic hydrolysis of (A) *p*-nitrophenyl sulfate, (B) ethyl *p*-nitrophenyl phosphate, (C) bis-*p*-nitrophenyl phosphate and (D) *p*-nitrophenyl phosphate. All free energy profiles and transition states correspond to a concerted A_ND_N mechanism, in which the phosphoryl/sulfuryl transfer and proton transfer from the nucleophile to the relevant base (see main text) occur in a single step. All ten profiles for the enzymatic reaction have been overlaid to demonstrate the convergence of the calculations. Additionally, the data for substrate (D) are based on our previous study [14].

Table S2, and the relevant energetics and a representative enzymatic transition state are shown in Table 1 and Fig. 2, respectively. From the table, it can be seen that, with this mechanism, we have reproduced the experimental activation barrier for *p*-nitrophenyl sulfate hydrolysis within an accuracy of 1 kcal/mol, with a standard deviation of 1.6 kcal/mol over 10 trajectories for the Lys113° case, which is preferred over $Lys113^+$ by ~3 kcal/mol. Finally, we obtain a calculated catalytic amplification of 11 kcal/mol (compared to the experimentally observed catalytic amplification of ~10.4 kcal/mol). Based on this, we propose a revised mechanism for the sulfuryl transfer reaction, in which His115 acts as a base to activate the nucleophile, and in which the sulfuryl transfer occurs in a concerted fashion with no leaving group protonation, resulting in a sulfo-enzyme intermediate.

3.2. Promiscuous phosphatase activity

PAS has been selected as our model system due to the fact that, in addition to sulfatase activity, it is also capable of promiscuous phosphatase activity [6], with proficiencies that can almost rival its native activity. Additionally, PAS shows greater proficiency towards a large bulky substrate such as bis-*p*-nitrophenyl phosphate

(BNPP), which has the same charge as the native substrate, than toward the smaller but dianionic *p*-nitrophenyl phosphate [6], suggesting an important role for electrostatics in determining the specificity, in line with the strong argument for the electrostatic basis for enzyme catalysis [17]. In order to verify this, we have examined the hydrolysis of two phosphodiesters by PAS, namely ethyl *p*-nitrophenyl phosphate (EpNPP) and bis-*p*-nitrophenyl phosphate (BNPP), both of which PAS catalyzes [6], but with an apparent preference for BNPP over EpNPP.

Fig. S5 shows an *ab initio* energy surface for EpNPP hydrolysis in aqueous solution, using acetaldehyde hydrate as a model for the formylglycine nucleophile. From this figure, it can be seen that the reaction follows a mechanism similar to that of hydroxide attack on analogous phosphodiesters [20], proceeding through a compact, concerted A_ND_N mechanism. Additionally, as with the corresponding monoester [8], the reaction proceeds via a substrate-as-base mechanism, with a non-bridging oxygen on the phosphate acting as the ultimate proton acceptor. Extrapolating from existing experimental data (see SI text) and using transition state theory gives an activation barrier of ~27.1 kcal/mol for the attack of the geminal diol on EpNPP, and, therefore, a $\Delta g^{\neq}_{cage}$ of ~24.7 kcal/mol for the reference reaction in solution, with which our calculated activation barrier (Table SI) is in good agreement. Therefore, we assume that a substrate-as-base mechanism is viable for both diesters, and that the activation barrier for this process can be extrapolated from existing experimental data, as outlined above, which, in the case of BNPP hydrolysis, suggests a $\Delta g^{\neq}_{cage}$ of ~26.9 kcal/mol for the reference reaction (see SI text). Based on this, we constructed the valence bond structures shown in Fig. S4, and performed EVB calculations, once again assuming a substrate-as-base mechanism with no protonation of the leaving group, similarly to the phosphate monoester [14]. The resulting free energy profiles and representative transition states are shown in Fig. 2. Based on the discussion above, one would expect catalytic amplifications of ~5.7 and 9.1 kcal/mol for EpNPP and BNPP hydrolysis respectively, and we obtain calculated amplifications of 4.2 and 10.2 kcal/mol respectively, with standard deviations of 0.3 kcal/mol over ten trajectories. This demonstrates that we not only reproduce the experimentally observed activation barriers, but also the difference in the relative catalytic proficiency towards the two diesters with high accuracy.

3.3. Lys113 as a specificity switch

A comparison of the obtained activation barriers for both the $Lys113^0$ and $Lys113^+$ cases for all substrates is presented in Table 1.[2] Both the sulfate monoester and the phosphodiesters, which are monoanionic, show a preference for $Lys113^0$. The impact on the diesterase activity is particularly dramatic, with $Lys113^+$ having a detrimental effect of up to 15.3 kcal/mol on the catalytic activity of the enzyme (Table 1). In contrast, for pNPP hydrolysis, neutralizing this residue results in unphysical results with extreme product trapping, emphasizing once again the importance of correct electrostatic treatments in simulation protocols. Clearly, more than four substrates are needed to ascertain a definitive trend, however it would appear that there is a correlation between the preferred ionization state of Lys113 and substrate charge, with this residue preferring to be neutral in the case of monoanionic substrates and ionized in the case of dianionic substrates (which in theory could help with the binding of the respective substrates). It is also worth commenting on the fact that the greater sensitivity of the phosphate than the sulfate monoesters to the ionization state of this residue could be tied to the fact that the former reactions appear to proceed through a substrate-as-base mechanism, where the interaction between Lys113 and the relevant non-bridging oxygen of the substrate becomes critical (particularly as this is the oxygen being protonated on the substrate), in contrast to the sulfate, which uses an enzymatic base.

3.4. Sulfuryl transfer: associative or dissociative?

Both our earlier comparative study of phosphoryl and sulfuryl transfer in aqueous solution [8] and Fig. 3 of the present work suggest that, in aqueous solution, sulfuryl transfer proceeds through a more expansive transition state than the analogous phosphoryl transfer reaction, whereas, as indicated in Table 2, PAS significantly reduces the barrier of a more associative sulfuryl transfer reaction, particularly in comparison to the corresponding phosphoryl transfer reactions. Therefore, we have also explored the effect of modeling the system as proceeding through a more "dissociative" transition state that is closer to the transition state observed on the *ab initio* surface shown in Fig. S3 in aqueous solution, with S–O distances of 2.50 and 2.33 Å to the leaving group (Table 2, see also the related case of the Ras-GAP system [21]). Fig. 3 outlines (a) a representative dissociative transition state for the sulfuryl transfer reaction, (b) an overlay of the calculated free energy profiles for the both the associative (blue) and dissociative (red) sulfuryl transfer reactions in the PAS active site (with the region corresponding to the transition state zoomed in on), and (c) an overlay of the relevant electrostatic group contributions to both associative and dissociative transition states calculated using the linear response approximation (LRA) [18], with the dissociative mechanism shown in red and the associative mechanism shown in solid blue. The calculated activation barriers are 18.8 and 26.3 kcal/mol in PAS and in solution respectively, representing a catalytic enhancement of 7.5 kcal/mol, compared to 11.0 kcal/mol for the more associative transition state, with, once again, a preference for $Lys113^0$ over $Lys113^+$. Here, the fact that we obtain less catalysis for the dissociative than the associative pathway need not a priori rule out a dissociative mechanism, as it is possible that our calculated activation barrier in aqueous solution is overestimated (and thus, that we have underestimated the chemical effect of including general base catalysis from the imidazole group). Additionally, the surface shown in Fig. S3 is quite flat, with the energy difference between the regions corresponding to the two pathways examined here being at most 1–2 kcal/mol. Therefore, the difference between these two transition states in aqueous solution would be negligible (as multiple pathways are possible on a flat surface). Our EVB calculations suggest that PAS shows a clear preference for an associative pathway, and the switch from a dissociative to an associative transition state in the enzyme active site is quite pronounced, particularly in light of the fact that even when modeling a more dissociative pathway in aqueous solution, we observe significant tightening of the corresponding enzymatic transition state (to a much greater extent than for any of the other reactions examined). Note that it has been argued that electrostatic interactions with positively charged active site residues do not tighten the transition state for phosphoryl transfer in the evolutionarily related active site of alkaline phosphatase [22]. However, this conclusion was drawn based on a comparison of data from examining linear free energy relationships (LFER), which are an extremely powerful component of the physical organic chemistry toolbox, but also very difficult to interpret qualitatively, as different pathways can give rise to similar LFER [23,24]. Therefore, similar LFER do not necessarily rule out a change of pathway. Additionally, it is worth mentioning at this stage some recent related theoretical calculation the name-giving member of the AP superfamily, alkaline phosphatase [25,26]. In both cases. authors focus on the promiscuous phosphodiesterase activity of AP.

[2] Note that the $Lys113^+$ results for the phosphate monoester dianion are from our previous work [13], and the corresponding $Lys113^0$ results were recalculated here, using the same protocol as for all other substrates.

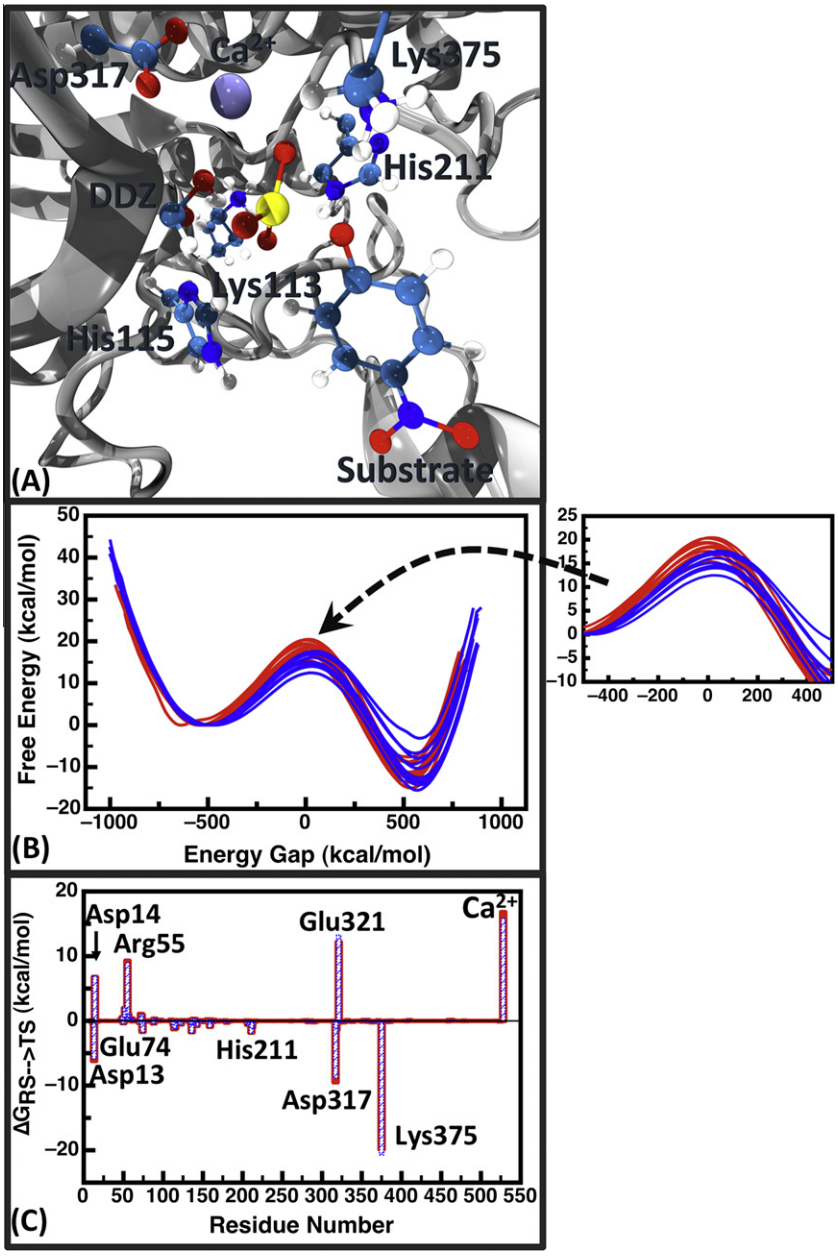

Fig. 3. (A) Representative transition state for sulfuryl transfer in the PAS active site, obtained when modeling the background reaction as a more dissociative process. (B) An overlay of activation barriers to "dissociative" (red) and "associative" (blue) sulfate hydrolysis, with the region surrounding the transition state zoomed in on for clarity, and (C) an overlay of the electrostatic group contributions to the calculated activation barrier for the dissociative (solid red) and associative (shaded blue) processes, averaged over ten trajectories.

Table 2
Average P(S)–O distances at the transition state for the relevant group transfer.[a]

Substrate[b]	Water		Enzyme		Difference	
	P(S)–O_{nuc}	P(S)–O_{lg}	P(S)–O_{nuc}	P(S)–O_{lg}	P(S)–O_{nuc}	P(S)–O_{lg}
(Ia)	2.257	2.001	2.150	1.979	−0.107	−0.022
(Ib)	2.504	2.328	2.348	2.199	−0.156	−0.129
(2)	2.466	2.356	2.320	2.307	−0.146	−0.049
(3)	2.470	2.349	2.401	2.280	−0.069	−0.069
(4)	2.443	2.272	2.350	2.234	−0.093	−0.038

[a] All distances are in Å, and averages over 10 trajectories.
[b] Shown here are (1a) *p*-nitrophenyl sulfate (associative pathway), (1b) *p*-nitrophenyl sulfate (dissociative pathway), (b) ethyl-*p*-nitrophenyl phosphate, (3) bis-*p*-nitrophenyl phosphate and (4) *p*-nitrophenyl phosphate.

However, in the first case [25], the authors obtain a transition state that is far more dissociative in the enzyme than in solution, which is counterintuitive in light of the presence of three divalent metal ions in active site, two of which are directly involved in the catalytic mechanism. It is worth nothing however, that the authors also observe an extreme increase in the distance between the catalytic metal centers of in excess of 5.5 Å for different WT and mutant forms of the enzyme, which clearly suggests a problem with the calculations (as was also commented on by [26]). Another recent work [26] also performed a detailed theoretical study of phosphodiester hydrolysis in the AP active site, demonstrating that the enzyme significantly tightens transition state in the AP active site compared to aqueous solution, and making the mechar far more associative as would be expected in the presence of multiple divalent metal ions, ar in line with the results presented here. However,

while the authors do try to calibrate 1 calculations to the corresponding reference reaction in solution, there is still significant variation in the obtained results, which may then be also the reason for the large error when comparing theory and experiment for the wild-type and mutant enzymes. Despite this, however, this is a very elegant work that highlights the importance of theoretical approaches in trying to rationalize enzyme catalysis.

3.5. A direct comparison of different substrates

Table 1 and Fig. 2 demonstrate that we can reproduce the catalytic effect of PAS with different substrates of interest with reasonable accuracy. On the one hand, PAS has a sufficie large binding pocket to allow it to accommodate a range of substrates of different sizes. However, it also appears to be very catalytically versatile, adapting not only the base depending on the specific substrate, but also electrostatically "self-regulating", with the ionization state of Lys113 appearing to play a role in determining the specificity. Additionally, while all substrates are hydrolyzed through a concerted A_ND_N process, the "size" of the transition state differs between them. Table 2 shows average distances at the transition state for each substrate in aqueous solution as well as in the corresponding enzyme catalyzed reaction, as well as the change in these distances upon moving from ground to transition state. Here, it can be seen that, in all cases, moving from aqueous solution to the enzyme involves a slight tightening of the transition state for the relevant reaction (see also [14]), as was also shown in the analogous case of phosphate diester hydrolysis by alkaline phosphatase [26]. However, the distribution of this tightening is not uniform across the four substrates, and the two substrates towards which PAS shows the highest catalytic activity (Table 1) proceed through both the most compact and the most expansive transition states of the series (Table 2), highlighting the fact that the specificity is not being determined by the size of the transition state. It has been repeatedly demonstrated (see e.g. [17]) that the main contributor to the tremendous catalytic proficiencies of enzymes is the electrostatic preorganization of the active site [27]. Additionally, the AP-superfamily provides an example of convergent evolution, since two significantly different active sites, one of which uses either Ser or Thr as a nucleophile and two metal ions (alkaline phosphatase and nucleotide pyrophosphatase/phosphodiesterase), and the other which uses a formylglycine (fGly) nucleophile and only one divalent metal ion (arylsulfatase and phosphonate monoester hydrolase), perform similar chemistry [4]. These observations suggest that the underlying basis for the inherent promiscuity for these types of reactions is determined by the requirements of the chemistry and most likely dominated by electrostatic interactions during the chemical step.

To explore this issue, we first examined the change in reorganization energy (λ) upon moving from aqueous solution to the PAS active site (Table 2). It can be seen that, in all cases, the reduction in λ, is smaller in the case of the promiscuous reactions compared to the native reaction, reflecting the fact that the enzyme has evolved to provide a maximally preorganized active site for its native reaction and not its promiscuous reactions. We then examined changes in electrostatic "group" contributions (i.e. the contributions of different residues) to the overall activation barrier for the enzyme-catalyzed reaction. This was done using the LRA, as in our previous work [14], and an overlay of the corresponding group contributions to the activation barrier for all substrates (averaged over all trajectories) is shown in Fig. 4. Note that, as discussed in [14] (and references cited therein), correct quantification of the metal cation is *extremely* challenging, therefore, the trend provided for the Ca^{2+} ion is only qualitative. However, despite the fact that the four substrates are hydrolyzed through "different" mechanisms, and that the preferred ionization state of Lys113

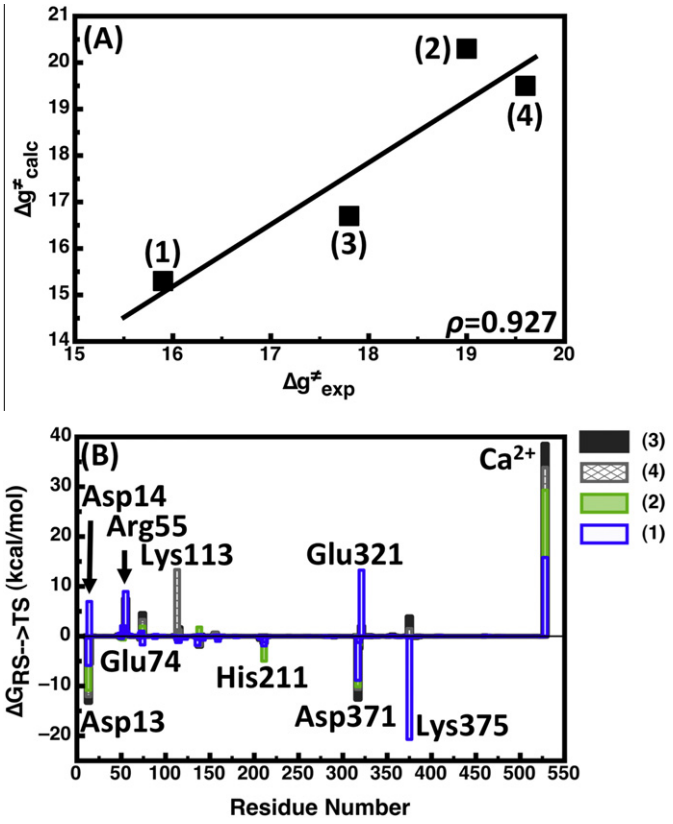

Fig. 4. (A) The correlation between experimental and calculated activation barriers for the hydrolysis of (1) *p*-nitrophenyl sulfate, (2) ethyl-*p*-nitrophenyl phosphate, (3) bis-*p*-nitrophenyl phosphate and (4) *p*-nitrophenyl phosphate. (B) An overlay of the electrostatic group contributions to the calculated activation barrier for each substrate, calculated using the LRA approach, with the raw data presented in tabulated form in Table S3.

changes depending on the substrate, the group contributions for the four substrates differ quantitatively, but qualitatively, they overlay almost perfectly. That is, the same key interactions appear to be involved for the native and promiscuous reactions, though interactions that are favorable for the native reaction are not necessarily also favorable for the promiscuous reaction (and, additionally, the deactivating effect of the calcium ion discussed in [14] is much smaller in the native than in the promiscuous reactions). This reflects the fact that the active site preorganization is suboptimal for the promiscuous substrates; however, it appears to be sufficiently flexible to allow for the catalysis of these chemically distinct reactions. Finally, note as an aside that in our previous work [14], we dissected the potential cause for the deactivating effect of the calcium ion, demonstrating that, while the calcium ion is deactivating for the overall reaction, it is nevertheless favorable for the initial proton transfer to the phosphate monoester. This reflects the fact that the proton is transferred directly to the non-bridging oxygen on the same face as the calcium ion, changing the phosphate from a dianion to a monoanion (or, in the case of the diesters, from a monoanionic to a neutral species). In contrast, in the case of the sulfuryl transfer, there is no protonation of any of the non-bridging oxygens, which affects the corresponding charge distribution at the transition state, and potentially accounts for the smaller deactivating effect of the calcium ion.

4. Discussion

While it is becoming increasingly evident that catalytic promiscuity plays an important role in the evolution of function

within enzyme superfamilies [1], the precise molecular basis for such promiscuous activity remains poorly understood. In a recent study, we performed a detailed theoretical examination of the promiscuous phosphomonoesterase activity of the arylsulfatase from *P. aeruginosa* (PAS) [14], demonstrating that, despite being a sulfatase, in it's promiscuous activity, this enzyme behaves like a "classical" phosphatase. In the present work, our aim has been to explore the molecular basis for the specificity and promiscuity of this enzyme, and we have therefore extended our previous study of the phosphomonesterase activity [14] to a range of sulfate and phosphate ester substrates. We demonstrate that, while all reactions proceed through a concerted A_ND_N pathway, the native and promiscuous substrates proceed through two chemically distinct mechanisms, utilizing either an active site histidine or the substrate itself as a base for the native and promiscuous activities respectively, with no apparent requirement for general-acid catalysis to protonate the *p*-nitrophenyl leaving group (Fig. S6, although this could be due to the highly activated nature of the leaving group). Additionally, for all substrates, the corresponding transition state is more compact in the enzyme active site than in aqueous solution, with this effect being most pronounced in the case of sulfuryl transfer. However, despite this chemical flexibility, overlaying the electrostatic contributions of different residues to the overall activation barrier for different substrates shows that, in all cases, the key residues providing the largest electrostatic contributions to the observed activation barrier are very similar for each substrate, and the difference is predominantly quantitative, where interactions that are favorable for the native reaction are not necessarily so for the promiscuous reactions. Finally, the largest difference between the different substrates appears to be in an active site lysine, Lys113, which interacts with the non-bridging oxygens of the substrate, and appears to act as a specificity switch between mono- and dianionic substrates. This is in line with the observation that the major contributor to the catalytic activity of enzymes comes from the electrostatic preorganization of the active site [17,27], suggesting that, in this specific case, the driving force for the catalytic diversity of the enzyme comes from the fact that the electrostatic environment of the active site is sufficiently flexible to allow for the catalytic requirements of multiple chemically distinct substrates, however, as it has been optimized for catalytic activity of the enzyme towards the native substrate, it is less proficient towards its promiscuous substrates. It is also interesting to observe that the requirement of an external base makes catalyzing sulfuryl transfer more demanding than phosphoryl transfer, and the promiscuous substrates, by being able to act as their own proton sinks, are operating through a chemically simplified (and therefore less catalytically challenging) version of the native reaction. PAS is a member of a highly promiscuous superfamily of enzymes, in which the native substrate for one family member is often found as a promiscuous side-reaction in another, and the promiscuity patterns in this superfamily are well characterized [4]. We demonstrate here that in the case of PAS, the promiscuity is driven by the "flexibility" in the electrostatic preorganization of the active site, which accommodated multiple chemically-distinct substrates in addition to the native substrate. When combined with the postulated importance of promiscuity in protein evolution, we believe that PAS provides a perfect example of chemistry-driven protein evolution, a feature that can be manipulated for the design of highly proficient artificial enzymes.

Acknowledgements

The authors thank the Swedish Research Council (SCLK, grant 2010-5026) and the BBSRC (BvL) for funding, as well as the PDC center for High Performance Computing at KTH and the National Supercomputer Center (NSC) at Linkoping University for access to computational resources. Thanks also go to Florian Hollfelder and the Hollfelder group (particularly Charlotte Miton, Christopher Bayer and Balint Kintses), as well as Johan Aqvist, David van der Spoel and Arieh Warshel for insightful discussion.

Appendix A. Supplementary data

Supplementary data associated with this article can be found, in the online version, at http://dx.doi.org/10.1016/j.febslet.2012.04.012.

References

[1] Khersonsky, O. and Tawfik, D.S. (2010) Enzyme promiscuity: a mechanistic and evolutionary perspective. Annu. Rev. Biochem. 79, 471–505.
[2] Jensen, R.A. (1976) Enzyme recruitment in evolution of new function. Annu. Rev. Microbiol. 30, 409–425.
[3] Roethlisberger, D. et al. (2008) Kemp elimination catalysts by computational enzyme design. Nature 453, 164–166.
[4] Jonas, S. and Hollfelder, F. (2009) Mapping catalytic promiscuity in the alkaline phosphatase superfamily. Pure Appl. Chem. 81, 731–742.
[5] Wolfenden, R. (2006) Degrees of difficulty of water-consuming reactions in the absence of enzymes. Chem. Rev. 106, 3379–3396.
[6] Babtie, A.C., Bandyopadhyay, S., Olguin, L.F. and Hollfelder, F. (2009) Efficient catalytic promiscuity for chemically distinct reactions. Angew. Chem. 48, 3692–3694.
[7] Olguin, L.F., Askew, S.E., O'Donoghue, A.C. and Hollfelder, F. (2008) Efficient catalytic promiscuity of an enzyme superfamily: an arylsulfatase shows a rate acceleration of 10^{13} for phosphate monoester hydrolysis. J. Am. Chem. Soc. 130, 16547–16555.
[8] Kamerlin, S.C.L. (2011) A theoretical comparison of *p*-nitrophenyl phosphate and sulfate hydrolysis in aqeuous solution: implications for enzyme catalyzed sulfuryl transfer. J. Org. Chem. 72, 9228–9238.
[9] Adamczyk, AJ. and Warshel, A. (2011) Converting structural information into an allosteric-energy-based picture for elongation factor Tu activation by the ribosome. Proc. Natl. Acad. Sci. USA 108, 9827–9832.
[10] Lee, F.S., Chu, Z.T. and Warshel, A. (1993) Microscopic and semimicroscopic calculations of electrostatic energies in proteins by the POLARIS and ENZYMIX programs. J. Comp. Chem. 14, 161–185.
[11] Warshel, A. (1991) Computer modeling of chemical reactions in enzymes and solutions, John Wiley & Sons, New York.
[12] Boltes, I. et al. (2001) 1.3A structure of arylsulfatase from *Pseudomonas aeruginosa* establishes the catalytic mechanism of sulfate ester cleavage in the sulfatase family. Structure 9, 483–491.
[13] Berman, H.M., Westbrook, J., Feng, Z., Gilliland, G., Bhat, T.N., Weissig, H., Shindyalov, IN. and Bourne, P.E. (2000) The Protein Data Bank. Nucleic Acids Res. 28, 235–242.
[14] Luo, J., van Loo, B. and Kamerlin, S.C.L. (2012) Examining the promiscuous phosphomonoesterase activity of *Pseudomonas aeruginosa* arylsulfatase: comparison to analogous phosphatases. Proteins: Struct. Funct. Bioinformat. 80, 1211–1226.
[15] Lee, F.S. and Warshel, A. (1992) A local reaction field method for fast evaluation of long-range electrostatic interactions in molecular simulations. J. Chem. Phys. 97, 3100–3107.
[16] Hengge, A.C. (2002) Isotope effects in the study of phosphoryl and sulfuryl transfer reactions. Acc. Chem. Res. 35, 105–112.
[17] Warshel, A., Sharma, P.K., Kato, M., Xiang, Y., Liu, H. and Olsson, M.H.M. (2006) Electrostatic basis for enzyme catalysis. Chem. Rev. 106, 3210–3235.
[18] Sham, Y.Y., Chu, Z.T., Tao, H. and Warshel, A. (2000) Examining methods for calculations of binding free energies: LRA, LIE, PDLD-LRA, and PDLD/S-LRA calculations of ligands binding to an HIV protease. Proteins: Struct. Funct. Genet. 39, 393–407.
[19] Sham, Y.Y., Chu, Z.T. and Warshel, A. (1997) Consistent calculations of pK_a's of ionizable residues in proteins: semi-microscopic and microscopic approaches. J. Phys. Chem. B 101, 4458–4472.
[20] Rosta, E., Kamerlin, S.C.L. and Warshel, A. (2008) On the interpretation of the observed linear free energy relationship in phosphate hydrolysis: a thorough computational study of phosphate diester hydrolysis in solution. Biochemistry 47, 3725–3735.
[21] Glennon, T.M., Villa, J. and Warshel, A. (2000) How does GAP catalyze the GTPase reaction of Ras? A computer simulation study. Biochemistry 39, 9641–9651.
[22] Nikolic-Hughes, I., Rees, D. and Herschlag, D. (2004) Do electrostatic interactions with positively charged active site groups tighten the transition state for enzymatic phosphoryl transfer? J. Am. Chem. Soc. 126, 11814–11819.
[23] Åqvist, J., Kolmodin, K., Florian, J. and Warshel, A. (1999) Mechanistic alternatives in phophsate monoester hydrolysis: what conclusions can be drawn from available experimental data? Chem. Biol. 6, R71–R80.

[24] Klähn, M., Rosta, E. and Warshel, A. (2006) On the mechanism of hydrolysis of phosphate monoesters dianions in solutions and proteins. J. Am. Chem. Soc. 128, 15310–15323.
[25] Lopéz-Canut, V., Roca, M., Bertrán, J., Moliner, V. and Tufñon, I. (2011) Promiscuity in alkaline phosphatase superfamily. Unraveling evolution through molecular simulations. J. Am. Chem. Soc. 133, 12050–12062.
[26] Hou, G. and Cui, Q. (2012) QM/MM analysis suggests that alkaline phosphatase and nucleotide pyrophosphatase/phosphodiesterase slightly tighten transition state for phosphate diester hydrolysis relative to solution. J. Am. Chem. Soc. 134, 229–246.
[27] Warshel, A. (1978) Energetics of enzyme catalysis. Proc. Natl. Acad. Sci. USA 75, 5250–5254.